Research on Chemical Intermediates
https://doi.org/10.1007/s11164-018-03715-x

Two novel fluorescent probes based on phenothiazine: synthesis and "naked-eye" colorimetric recognition of Hg^{2+}

Chuane Wang[1] · Lizhen Wang[2] · Shimin Fang[1] · Dawei Qin[1] · Jianhua Zhou[1] · Geng Yang[1] · Shuangshuang Jin[1] · Hongdong Duan[1]

Received: 10 October 2018 / Accepted: 14 December 2018

Abstract

Two novel colorimetric and fluorescent probes 2-(1,3-dithiolanes)-10-ethyl phenothiazine (**PHE–Ed**) and 2-(1,3-dithianes)-10-ethyl phenothiazine (**PHE–Pd**) based on phenothiazine were successfully synthesized, and their structure was confirmed by NMR and high resolution mass spectra. Fluorescence investigations revealed that the synthesized probes could be used for the selective detection of Hg^{2+}, which was accompanied with an obvious color change from colorless to light yellow. The applicable ability of the two probes was investigated by a series of competitive experiments, solid colorimetric experiments, and applied experiments, which proved that these probes showed high sensitivity and great potential to detect Hg^{2+} in environmental analysis systems. Furthermore, the detection mechanism of the probes was investigated by FT-IR spectra and NMR spectra, and the results indicated that the detection of Hg^{2+} was accomplished through the Hg^{2+}-promoted deprotection of thioacetal.

Keywords Phenothiazine · 1,2-ethanedithiol · 1,3-propanedithiol · ICT fluorophore · Naked-eye

Introduction

Nowadays, the manufacture and use of mercury has dramatically increased, due to its wide application in industry [1, 2]. Mercury is hardly biodegradable and can be biomagnified in the food chain, thereby causing serious human health problems, including digestive, cardiac, kidney and DNA damage, mitosis impairment,

✉ Hongdong Duan
hdduan67@163.com

[1] School of Chemistry and Pharmaceutical Engineering, Qilu University of Technology, (Shandong Academy of Sciences), Jinan 250353, Shandong Province, China

[2] Biology Institute, Qilu University of Technology (Shandong Academy of Sciences), Jinan 250014, Shandong Province, China

Published online: 04 January 2019

and permanent damage to the central nervous system [3, 4]. Therefore, the development of a highly efficient and novel strategy for detection of Hg^{2+} ion is important for both human health and the environment.

Many fluorescent probes based on fluorescence turn-on or turn-off sensing mechanisms have been developed for the detection of Hg^{2+}. However, these strategies have so many limitations, because the fluorescence signal intensity is very sensitive and susceptible to external factors, such as temperature, excitation power, media properties, etc. [5, 6]. To solve this problem, a new type of fluorescent probe based on the Hg^{2+}-induced chemical reactions has been developed. These probes can detect Hg^{2+} with high selectivity and fluorescence intensity enhancement, and simultaneously producing obvious color changes [7]. More importantly, these probes, with high chemoselectivity toward Hg^{2+}, are hardly affected by the external factors. Consequently, these reaction-based probes are superior to other fluorescence detection methods in terms of the sensitivity and selectivity, and have been widely applied for the detection of Hg^{2+} [8, 9].

Phenothiazine (PHE) derivatives have a long history, with successive periods of interest in different areas of applied chemistry, such as dyes, probes, pharmaceuticals, and electrochemistry [10–14]. PHE can provide strong fluorescence, structural regulation, good hole transport capacity, and low ionization potential. Therefore, PHE derivatives can be used as raw materials for the development of various fluorescent probes [15]. This paper reported the synthesis of two colorimetric fluorescent probes **PHE–Ed** and **PHE–Pd** based on phenothiazine as shown in Scheme 1. These two probes could be used for the high selective signaling of Hg^{2+} ions through Hg^{2+}-induced deprotection of dithioacetal, and this deprotection reaction produced an aldehyde and exhibited pronounced fluorescence enhancement [16–18]. Moreover, an obvious color change of the solution from colorless to light yellow could be observed, indicating its potential application for the naked–eye detection of Hg^{2+} ions [19–25].

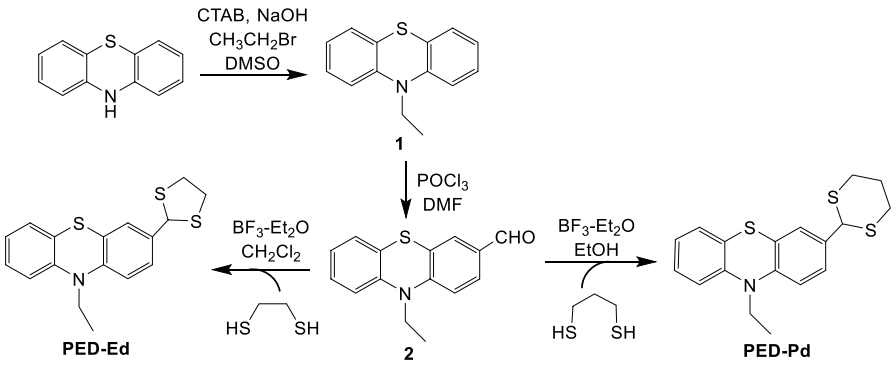

Scheme 1 Synthesis of sensors **PHE-Ed** and **PHE-Pd**

Experimental

Materials and instrumentation

All solvents and chemicals (analytical grade) were obtained from commercial suppliers and used without further purification. The laboratory used TLC to detect the reaction process. Fourier Transform Infrared (FTIR) spectra were obtained by using KBr pellets on a TENSOR27 FT–IR spectrometer. The NMR spectra were analyzed on a Bruker Avance 400 Spectrometer using dimethyl sulfoxide (DMSO–*d6*) as the solvent, and chemical changes were recorded in ppm using tetramethylsilane (TMS) as an internal standard. High resolution mass spectra (HRMS) were carried out using an Agilent 6510 Accurate–Mass Q–TOF LC/MS system. The fluorescence data were obtained by a F–4500 (Hitachi) fluorescence spectrometer.

Synthesis and characterization

Synthesis of compound 1

To the mixture of phenothiazine (3.986 g, 20.0 mmol), NaOH (6.40 mL, 79.5 mmol) and CTAB (0.200 g, 0.5 mmol) in 50 mL of DMSO was slowly added ethyl bromide (2.178 g, 20.0 mmol), and then the reaction was allowed to warm to 35 °C and stirred at ambient temperature for 6 h. After TLC showed the conversion of the starting material, the above mixture was cooled to room temperature, and distilled (150 mL) water was added. The mixture was then extracted three times with ethyl acetate (150 mL × 3), the organic layer was then evaporated and the resultant residue was purified by column chromatography (petroleum ether/dichloromethane 10/1) to provide compound 1 as white crystals (3.520 g, yield 77%); M.p. 103.3–103.7 °C; IR (KBr, cm^{-1}) 2907 (CH_3), 1639 (C=C), 1442 (C=C), 1236 (C–N), 1108 (C–S) cm^{-1}; ^1H NMR (400 MHz, DMSO–d_6) δ = 7.2–27.17 (m, 2 H), 7.14 (d, J = 7.6 Hz, 2 H), 7.01 (d, J = 7.4 Hz, 2 H), 6.94 (t, J = 7.5 Hz, 2 H), 3.91 (s, 2 H), 1.29 (s, 3 H); ^{13}C NMR (101 MHz, DMSO–d_6) δ = 144.88, 128.06, 127.47, 123.47, 122.82, 115.92, 13.15; ESI-TOF HRMS (*m/z*): calcd for $C_{14}H_{13}SN$, $[M+H]^+$, 227.0918; found, 227.0912.

Synthesis of compound 2

Phosphorus oxychloride (1.90 mL, 20.0 mmol) was slowly added to 5 mL of dry DMF at 0 °C, and the mixture was warmed to room temperature and stirred for 1 h. Then, a solution of 10-ethyl phenothiazine (2.273 g, 10.0 mmol) in 20 mL of DMF was slowly added to the above mixture, and the reaction was heated to reflux for 12 h. After which, distilled water (100 mL) was added, and the reaction was neutralized with saturated NaOH aqueous solution. Then, the mixture was extracted three times with dichloromethane (150 mL × 3), the organic layer was collected and evaporated. The resultant residue was purified by column chromatography (petroleum

ether/ethyl acetate 4/1) to give compound **2** as yellow crystals; (1.852 g, yield 72%); M.p. 97.9–98.2 °C; IR (KBr, cm^{-1}) 2907 (CH_3), 1671 (CHO), 1609 (C=C), 1462 (C=C), 1202 (C–N), 1104 (C–S) cm^{-1}; ^1H NMR (400 MHz, DMSO–d_6) δ = 9.65 (s, 1 H), 7.65–7.39 (m, 2 H), 7.18–6.84 (m, 5 H), 3.87 (s, 2 H), 1.18 (s, 3 H). ^{13}C NMR (101 MHz, DMSO–d_6) δ = 190.99, 149.96, 143.02, 131.22, 130.71, 128.45, 128.03, 127.60, 124.00, 123.27, 122.23, 116.55, 115.54, 13.06; ESI-TOF HRMS (*m/z*): calcd for $C_{15}H_{13}SNO$, $[M+H]^+$, 255.0812; found, 255.0815.

Synthesis of PHE–Ed

To the mixture of 2-aldehyde-10-ethyl phenothiazine (0.205 g, 1.0 mmol) and 1,2-ethanedithiol (0.092 g, 1.0 mmol) in 20 mL of dichloromethane was added a catalytic amount of boron trifluoride diethyl etherate (0.10 mL, 0.79 mmol) at 0 °C. The reaction was stirred at 0 °C overnight, and 10 mL of methanol was added. After which, a pale green precipitate was formed, the mixture was then filtered and the solid was washed with methanol for three times to afford the desired product as green crystals (0.253 g, yield 61.8%); M.p. 83.4–84.7 °C; IR (KBr, cm^{-1}) 2906 (CH_3), 1637 (C=C), 1455 (C=C), 1211 (C–N), 1107 (C–S) cm^{-1}; ^1H NMR (400 MHz, DMSO–d_6) δ = 7.18 (dd, J = 8.4, 2.2 Hz, 1 H), 7.13 (d, J = 2.1 Hz, 1 H), 7.09–7.02 (m, 1 H), 6.99 (dd, J = 7.6, 1.5 Hz, 1 H), 6.87 (d, J = 8.1 Hz, 1 H), 6.80 (dt, J = 7.5, 3.2 Hz, 2 H), 5.54 (s, 1 H), 3.75 (q, J = 6.8 Hz, 2 H), 3.48–3.27 (m, 2 H), 3.23–3.12 (m, 2 H), 1.14 (t, J = 6.9 Hz, 3 H); ^{13}C NMR (101 MHz, DMSO–d_6) δ = 144.58, 144.40, 135.23, 128.16, 127.66, 127.50, 126.68, 123.30, 122.93, 115.91, 115.57, 54.65, 13.07; ESI-TOF HRMS (*m/z*): calcd for $C_{17}H_{17}S_3NO$, $[M+H]^+$, 331.0613; found, 331.0615.

Synthesis of PHE–Pd

To the mixture of 2-aldehyde-10-ethyl phenothiazine (0.205 g, 1.0 mmol) and 1,3-propanedithiol (0.108 g, 1.0 mmol) in 20 mL of ethanol was added a catalytic amount of boron trifluoride diethyl etherate (0.10 mL, 0.79 mmol), and the reaction was heated to reflux for 12 h. After TLC showed the conversion of the starting material, the reaction was cooled in a refrigerator and a pale pink solid was formed. The mixture was then filtered and the solid was recrystallized with acetonitrile to afford the desired product as white crystals (0.223 g, yield 64.5%); M.p. 129.5–130.1 °C; IR (KBr, cm^{-1}) 2939 (CH_3), 1602 (C=C), 1463 (C=C), 1240 (C–N), 1035 (C–S) cm^{-1}; ^1H NMR (400 MHz, DMSO–d_6) δ = 7.13–7.03 (m, 2 H), 7.03–6.97 (m, 2 H), 6.90–6.77 (m, 3H), 5.17 (s, 1 H), 3.76 (q, J = 6.8 Hz, 2 H), 2.91 (t, J = 12.4 Hz, 2 H), 2.73 (d, J = 14.0 Hz, 2 H), 1.97 (d, J = 14.0 Hz, 1 H), 1.55 (q, J = 12.6, 11.2 Hz, 1 H), 1.15 (t, J = 6.9 Hz, 3H). ^{13}C NMR (101 MHz, DMSO–d_6) δ = 144.74, 144.46, 134.08, 128.21, 127.52, 127.37, 126.31, 123.47, 123.02, 122.82, 115.93, 49.26, 31.51, 25.14, 13.06; ESI-TOF HRMS (*m/z*): calcd for $C_{18}H_{19}S_3NO$, $[M+H]^+$, 345.0811; found, 345.0814.

Result and discussion

Selectivity studies

UV–Vis absorption spectra

To investigate the recognition abilities of synthetic probes **PHE–Ed** and **PHE–Pd** toward Hg^{2+}, we carried out a series of host–guest recognition experiments on UV–Vis spectroscopy. As shown in Fig. 1, the recognition profiles of PHE–Ed

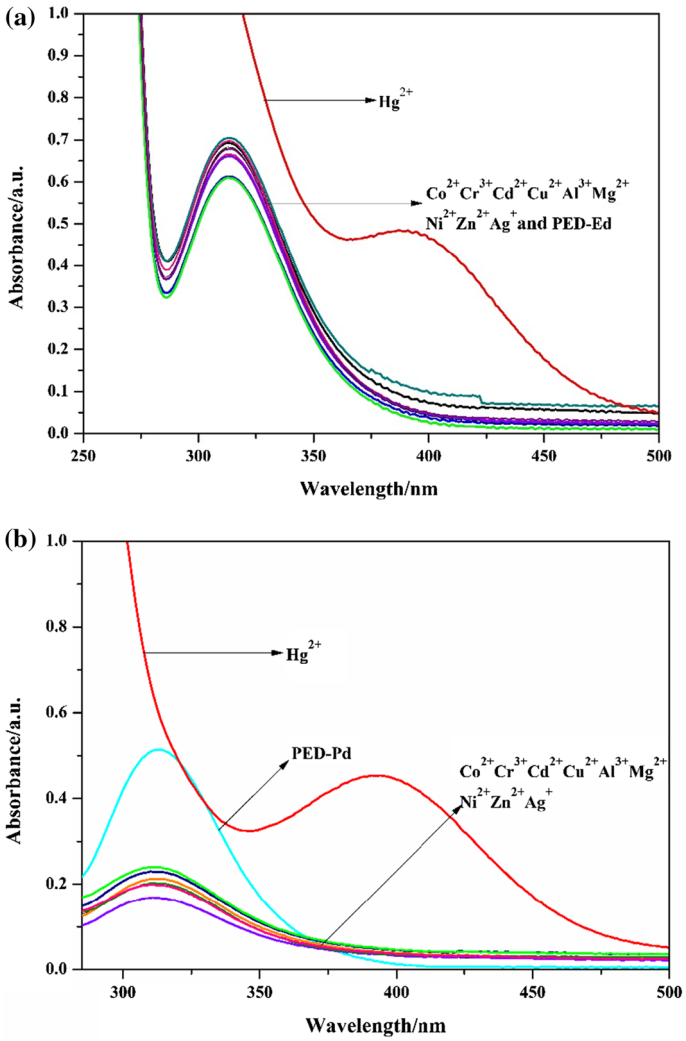

Fig. 1 **a** Absorption spectrum changes of sensor **PED–Ed** (10^{-5} M) in the presence of different metal ions (10^{-5} M) in EtOH/H_2O (1/1, v/v) solution; **b** Absorption spectrum changes of sensor **PED–Pd** (10^{-5} M) in the presence of different metal ions (10^{-5} M) in EtOH/H_2O (1/1, v/v) solution

toward various metal ions, including Ag^{+}, Mg^{2+}, Cd^{2+}, Al^{3+}, Co^{2+}, Ni^{2+}, Cu^{2+}, Zn^{2+} $Cr^{2+}$and Hg^{2+} were investigated in EtOH/H_2O (1/1, v/v) solution, and the results indicated that free probe **PHE–Ed** in EtOH/H_2O (1/1, v/v) solution exhibited an obvious absorption band at 310 nm (Fig. 1a). While addition of Hg^{2+} to the above solution containing free probe **PHE–Ed** resulted in a remarkable red–shift absorption band at 390 nm, indicating the coordination of probe **PHE–Ed** with Hg^{2+} ion. More importantly, this process was accompanied with an obvious color change from colorless to light yellow (Fig. 2a). In comparison, addition of other metal ions showed no significant change of the absorption band and color, indicating the high selectivity of probe **PHE–Ed** toward Hg^{2+} ion. The recognition profiles of **PHE–Pd** toward various metal ions were also investigated, and the similar absorption band shift (Fig. 1b) and color change (Fig. 2b) were observed after addition of Hg^{2+} ion to the solution containing free probe **PHE–Pd**. These results illustrated the high efficient and selectivity of **PHE–Pd** toward Hg^{2+} ion compared with various other metal ions including Ag^{+}, Mg^{2+}, Cd^{2+}, Al^{3+}, Co^{2+}, Ni^{2+}, Cu^{2+}, Zn^{2+} and Cr^{3+}. Next, Job's plots were used to determine the stoichiometries of the complexes formed between **PHE–Ed** and Hg^{2+}. The results indicated a 1:1 stoichiometry for the binding of probe **PHE–Ed** with Hg^{2+} (Fig. 3a). Furthermore, the association constant *K*a for the **PHE–Ed** with Hg^{2+} was calculated to be 9.6×10^{3} M^{-1} using the Benesi-Hildebrand equation. Similarly, the binding of probe **PHE–Pd** with Hg^{2+} was 1:1 and the association constant *K*a for the **PHE–Pd** with Hg^{2+} was determined as 1.23×10^{4} M^{-1} (Fig. 3b).

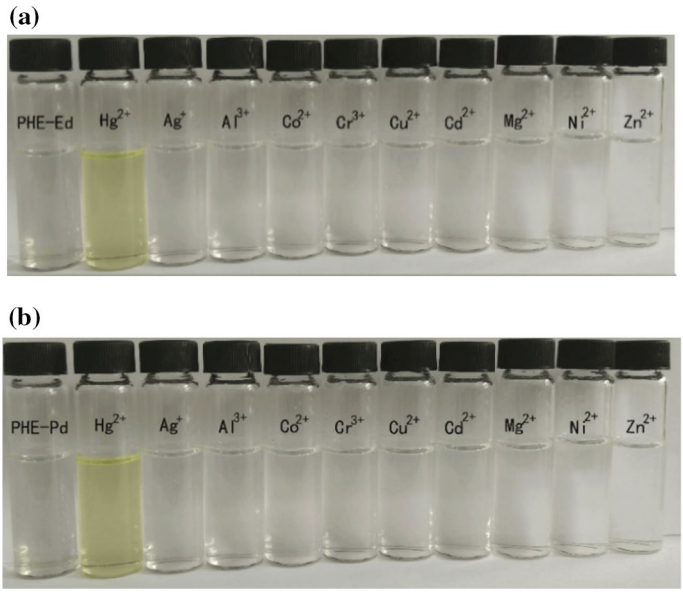

Fig. 2 **a** Colorimetric performance of sensor **PHE–Ed** (10^{-5} M) upon addition of different metal ions (10^{-5} M) in EtOH/H_2O (1/1, v/v) solution; **b** Colorimetric performance of sensor **PHE–Pd** (10^{-5} M) upon addition of different metal ions (10^{-5} M) in EtOH/H_2O (1/1, v/v) solution

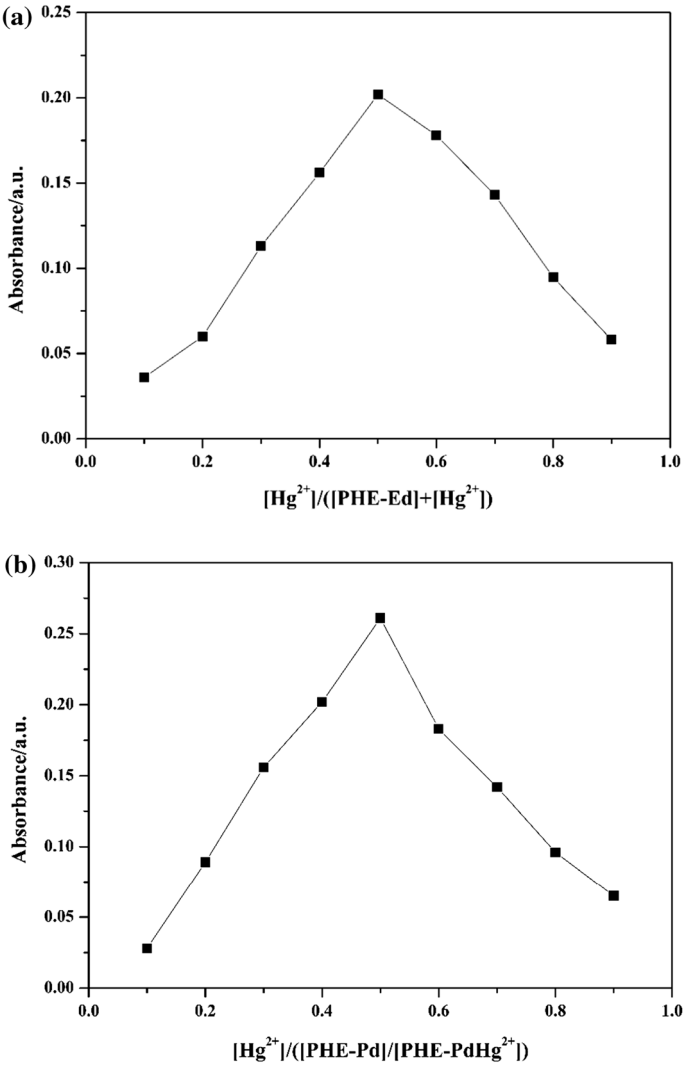

Fig. 3 **a** Job's plot for determining the stoichiometry of **PED–Ed** and Hg^{2+} in EtOH/H_2O (1/1, v/v) solution; **b** Job's plot for determining the stoichiometry of **PED–Pd** and Hg^{2+} in EtOH/H_2O (1/1, v/v) solution. The total concentration was 10 μM

Fluorescence spectra

The fluorescence spectra of probes **PHE–Ed** and **PHE–Pd** toward a series of metal ions (Ag^{+}, Mg^{2+}, Cd^{2+}, Al^{3+}, Co^{2+}, Ni^{2+}, Cu^{2+}, Zn^{2+}, Cr^{3+}, and Hg^{2+}) were studied in EtOH/H_2O (1/1, v/v) solution, as shown in Fig. 4. When at an excited wavelength of 390 nm was added Hg^{2+} ion to the solution containing free probe **PHE–Ed**, there resulted distinguished changes with a maximal fluorescence emission band at around 610 nm (Fig. 4a). However, addition of other

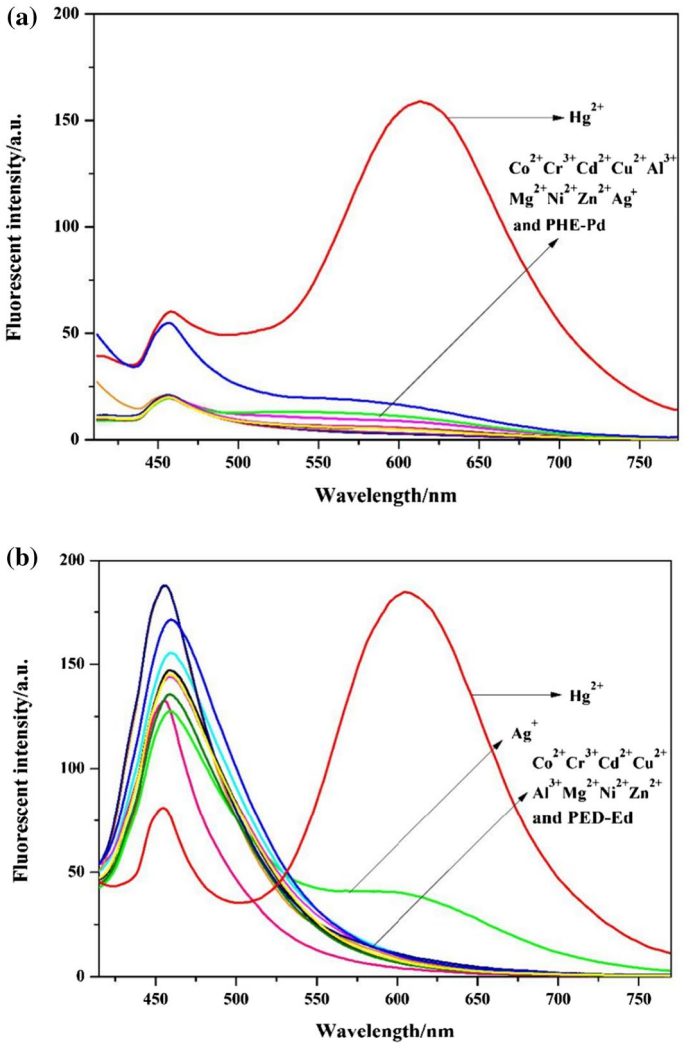

Fig. 4 **a** Fluorescence spectra response of sensor **PHE–Ed** (10^{-5} M) upon addition of different metal ions in EtOH/H_2O (1/1, v/v) solution; **b** Fluorescence spectra response of sensor **PHE–Pd** (10^{-5} M) upon addition of different metal ions in EtOH/H_2O (1/1, v/v) solution

metal ions to the above solution showed a fluorescence emission band at around 455 nm, which proved the high efficiency and selectivity of probe **PHE–Ed** toward Hg^{2+}. Similarly, a maximal fluorescence emission band at around 610 nm (Fig. 4b) was observed after addition of Hg^{2+} ion to the solution containing free probe **PHE–Pd**, and addition of other metal ions showed a fluorescence emission band at around 455 nm, which illustrated the high efficiency and selectivity of probe **PHE–Pd** toward Hg^{2+} ion. Furthermore, the quantum yields (Φ) of probes **PHE–Ed** and **PHE–Pd** were 0.11 and 0.12, respectively, using Rhodamine

B as reference, which proved the potential application of probes **PHE–Ed** and **PHE–Pd**.

Sensitivity studies

The sensitivity of PHE–Ed and PHE–Pd for detection of Hg^{2+}

To ascertain the sensitivity of probes PHE–Ed and PHE–Pd toward Hg^{2+}, the fluorescence titration experiments were performed in EtOH/H_2O (1/1, v/v) solution. As shown in Figs. 5 and 6, upon addition of an increasing amount of Hg^{2+} (0–14 μM) to the solution containing free probe PHE–Ed, a gradual increase of the emission peak could be observed around 610 nm, and the fluorescence intensity reached the platform when the concentration of Hg^{2+} was 10 μM, which implied the 1:1 response of PHE–Ed to Hg^{2+} (Fig. 5a). In addition, the fluorescence intensity enhancement showed a good linear relationship over Hg^{2+} ($R^2 = 0.99973$) (Fig. 5b), and the detection limit of PHE–Ed toward Hg^{2+} was determined to be as low as 1.87×10^{-8} mol/L on the basis of $3\sigma/k$, indicating high sensitivity of probe PHE–Ed for quantitative determination of Hg^{2+}. Similarly, addition of an increasing amount of Hg^{2+} (0–14 μM) to the solution of PHE–Pd (10 μM) also led to a gradual increase of the emission peak around 610 nm with about 16–fold of fluorescence intensity enhancement (Fig. 6a), and the fluorescence intensity enhancement was observed with a good linear relationship over the Hg^{2+} ($R^2 = 0.99764$) (Fig. 6b). Furthermore, the detection limit of PHE–Pd for Hg^{2+} was 2.07×10^{-8} mol/L on the basis of $3\sigma/k$. All these results indicated that probe PHE–Pd could be applied for determination of Hg^{2+} with high efficiency and sensitivity.

Detection mechanism

As shown in Scheme 2, Hg^{2+}–induced deprotection of thioacetals can lead to the formation of the corresponding aldehydes that other metal ions could not -induced deprotection reaction of thioacetals, consequently this process is always applied for the development of some reaction–based probes to detect Hg^{2+} ion. In probes **PHE–Ed** and **PHE–Pd**, the electron–rich 2-ethyl phenothiazine group was designed as electron donor, and the dithioacetal group was designed as a weak electron donor, which formed a donor–donor system to suppress the intramolecular charge transfer (ICT) process. When Hg^{2+} ion was added to the solution containing free **PHE–Ed** and **PHE–Pd**, respectively, an electron–deficient aldehyde group was formed. This aldehyde group could be served as an electron acceptor and combined with the electron–rich group (2–ethyl phenothiazine) to switch on the ICT process, thereby causing a significant red shift in the absorption and emission bands [26–32].

To further confirm the detection mechanism of probes **PHE–Ed** and **PHE–Pd**, the reaction product of probe **PHE–Ed** and **PHE–Pd** with Hg^{2+} has been confirmed by the FT-IR spectra. As shown in Fig. 7a, the FT-IR spectra of **PHE–Ed** in the presence of Hg^{2+} (1.0 equiv) clearly showed a new typical and prominent

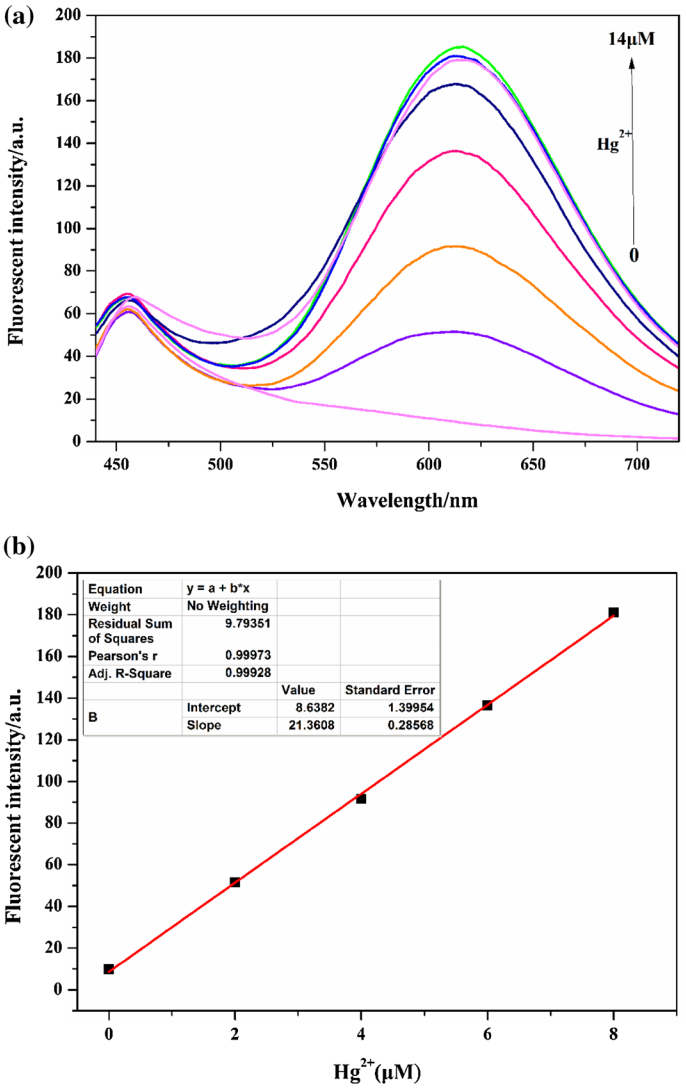

Fig. 5 **a** The fluorescence spectra of sensor **PHE–Ed** (10 μM) with the increasing concentration of Hg^{2+} ions (0–14 μM) in EtOH/H_2O (1/1, v/v) solution; **b** The linear fit between sensor **PHE–Ed** and Hg^{2+} ions

absorption peak of an aldehyde group at 1665 cm^{-1}, which indicated the successful deprotection of a dithioacetal group induced by Hg^{2+}. Similarly, the FT-IR spectra of **PHE–Pd** in the presence of Hg^{2+} (1.0 equiv) showed a new typical and prominent absorption peak of an aldehyde group at 1684 cm^{-1} as shown in Fig. 7b, which proved the successful deprotection of the dithioacetal group.

Moreover, the ^{1}HNMR titration experiments were implemented to measure the deprotection process. As shown in Fig. 8a, after addition of Hg^{2+} ion (10 μM) to the solution of PHE–Ed (10 μM) in DMSO–d_6, the original signal assigned

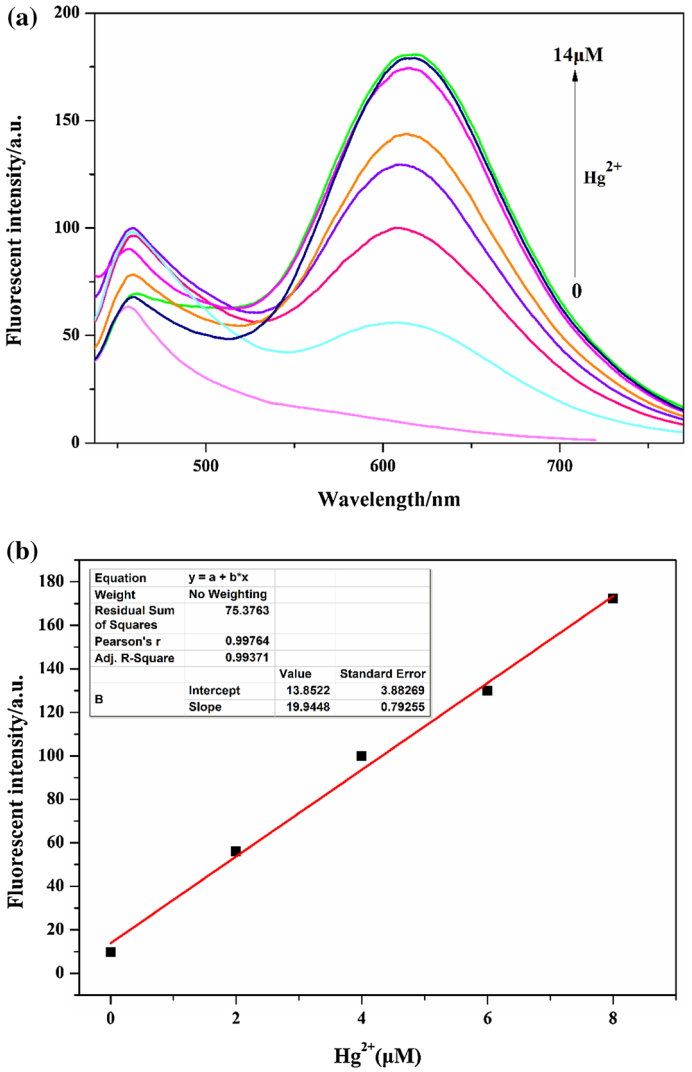

Fig. 6 **a** The fluorescence spectra of sensor **PHE–Pd** (10 uM) with the increasing concentration of Hg^{2+} ions (0–14 μM) in EtOH/H_2O (1/1, v/v) solution; **b** The linear fit between sensor **PHE–Pd** and Hg^{2+} ions

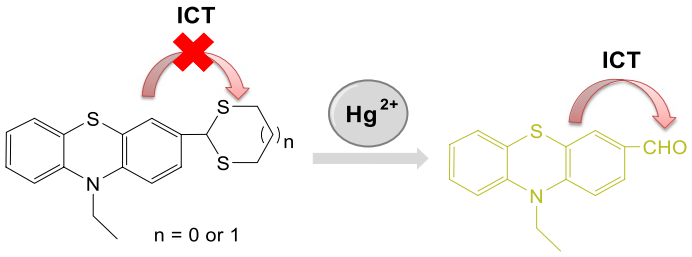

Scheme 2 The proposed sensing mechanism of sensor **PHE–Ed** and **PHE–P**d toward Hg^{2+}

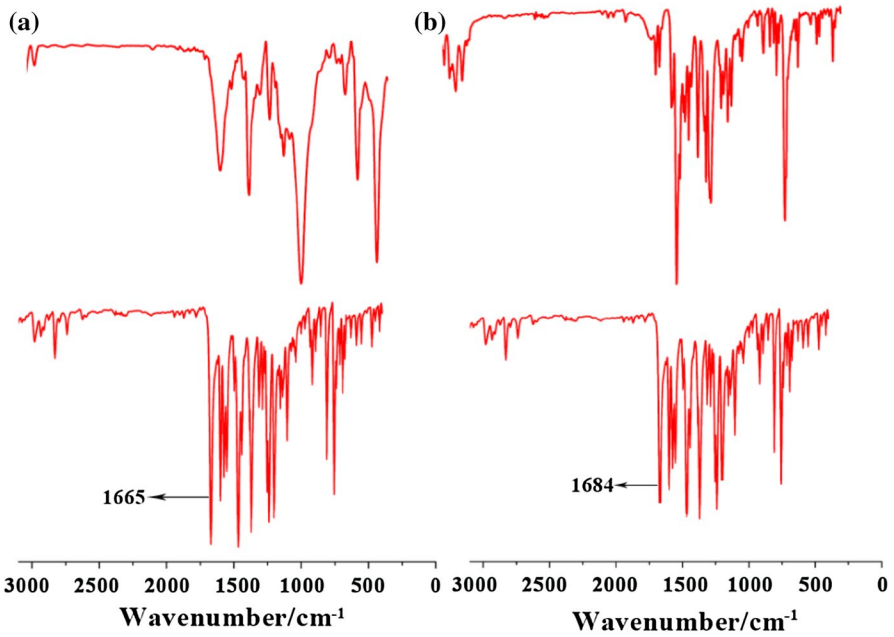

Fig. 7 **a** FT-IR spectra of Hg^{2+} ions (10 μM) to **PHE–Ed** (10 μM) in EtOH/H_2O (1/1, v/v) solution; **b** FT-IR spectra of Hg^{2+} ions (10 μM) to **PHE–Pd** (10 μM) in EtOH/H_2O (1/1, v/v) solution

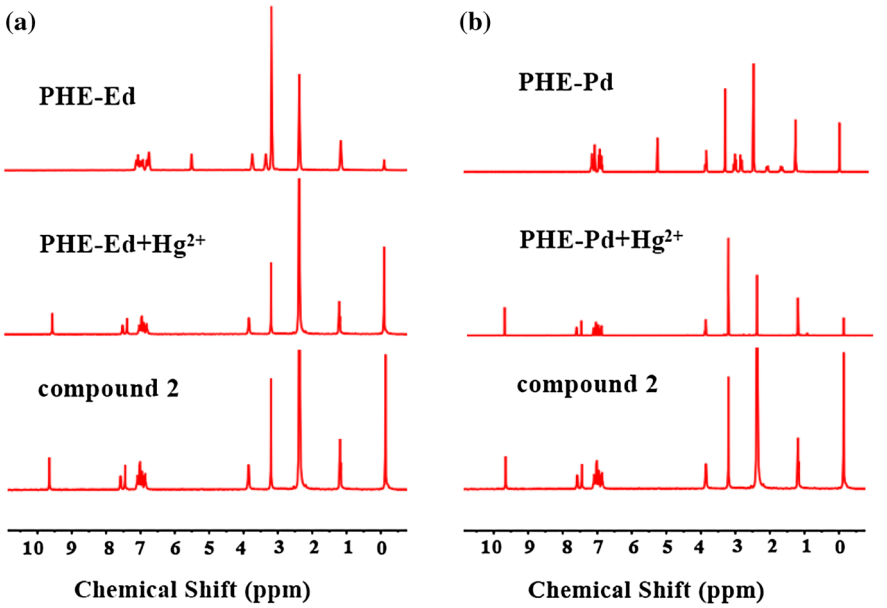

Fig. 8 **a** ^1H NMR spectra of Hg^{2+} ions (10 μM) to **PHE–Ed** (10 μM) in DMSO–d6; **b** ^1H NMR spectra of Hg^{2+} ions (10 μM) to **PHE–Ed** (10 μM) in DMSO–d6

to the methane (CH) proton at 5.54 ppm, and two other signals at 3.48–3.27 and 3.23–3.12 ppm assigned to methylene (CH_2CH_2) protons of the thioacetal group disappeared completely. Concomitantly, a new peak at 9.65 ppm corresponding to the aldehyde proton appeared, indicating the successful removal of the thioacetal group. Similarly, the ^{1}HNMR spectrum of PHE–Pd also dramatically changed after addition of Hg^{2+} ions, as shown in Fig. 8b. For example, the original signal ascribed to the methane (CH) proton (5.17 ppm) and the original signals assigned to the methylene (CH_2–CH_2–CH_2) protons (2.91, 2.73, 1.97 and 1.55 ppm) all disappeared completely. At the same time, a new peak at 9.80 ppm corresponding to the aldehyde

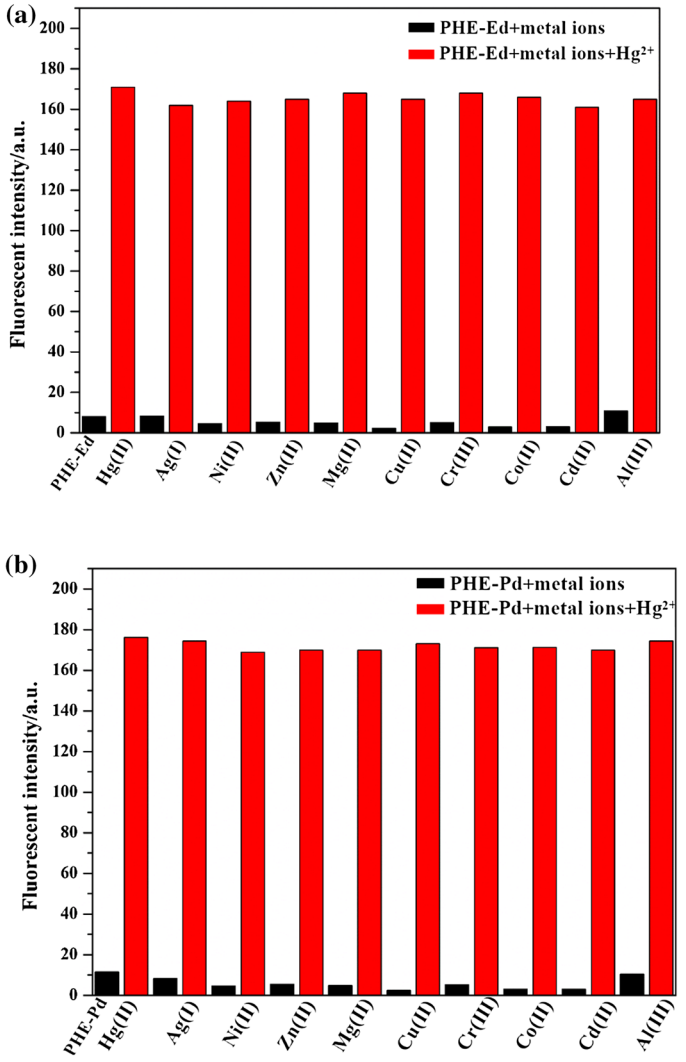

Fig. 9 The anti–interference properties of sensor **PHE–Ed** and **PHE–Pd** toward Hg^{2+} upon addition of different metal ions (10^{-5} M) in EtOH/H_2O (1/1, v/v) solution

proton appeared. The two newly formed ^{1}HNMR spectra were both nearly or the same as that of compound **2**, indicating the successful deprotection of dithioacetal groups in **PHE–Ed** and **PHE–Pd** triggered by Hg^{2+}.

Anti–interference Properties

The selectivity of probes **PHE–Ed** and PHE–Pd toward Hg^2 were investigated by a series of competitive experiments in EtOH/H_2O (1/1, v/v) solution (Fig. 9a). Upon mixing of probe **PHE–Ed** (10 μM) with other metal ions (Ag^+, Mg^{2+}, Cd^{2+}, Al^{3+}, Co^{2+}, Ni^{2+}, Cu^{2+}, Zn^{2+}, Cr^{3+}), the fluorescence intensity at 610 nm showed no distinguishing changes. Subsequent addition of Hg^{2+} to the above solution led to a prominent enhancement of the emission band at 610 nm, which demonstrated that probe PHE–Ed showed high selectivity for detecting Hg^{2+} ion. A similar phenomenon was observed in the competitive experiment of probe **PHE–Pd** (10 μM) with various metal ions (Fig. 9b), and the results indicated that probe PHE–Pd exhibited high selectivity and anti–interference ability toward Hg^{2+}.

The pH Effects and sensing response time

The influence of pH and response time on fluorescence properties was investigated in EtOH/H_2O (1/1, v/v) solution. Probes PHE–Ed and PHE–Pd were treated with Hg^{2+} (10 μM) in a wide pH range of 2.0–12.0 as shown in Fig. 10a, and an obvious fluorescence enhancement was observed in the pH range of 5.0–9.0, which illustrated that the two probes showed high detection abilities in the middle pH value. Furthermore, the time required for Hg^{2+}-promoted deprotection of PHE–Ed and PHE–Pd was measured in EtOH/H_2O (1/1, v/v) solution as shown in Fig. 10b. Upon treatment of the two probes with Hg^{2+} (10 μM), the fluorescence intensity obviously enhanced with the increasing of time, and reached a platform after 5 min later. These results revealed that the two colorimetric fluorescent probes can quickly identify Hg^{2+} in 5 min and meet the response time requirements for real–time monitoring of Hg^{2+} with high sensitivity and selectivity in practical samples.

Research on solid colorimetric experimental and practical application

To confirm whether probes **PHE–Ed** and **PHE–Pd** can be used as simple and efficient solid–state fluorescent probes for detecting Hg^{2+}, the recognition ability of the two synthetic probes toward Hg^{2+} was determined on pretreated filter paper strips, as shown in Fig. 11. The filter paper strips were placed in solution of **PHE–Ed** or **PHE–Pd** (1.0×10^{-3} mol/L) in DMSO for several seconds and then removed. The test strips were dried in air and then treated with Hg^{2+} solution (1.0×10^{-5} mol/L) in water. When the test strips were dipped into the solution of Hg^{2+}, all strips demonstrated distinct color changes. These results proved that the probes PHE–Ed and PHE–Pd could be applied for the solid–state detection of Hg^{2+}, thus providing a convenient, economical and highly efficient method for naked–eye detection of Hg^{2+}.

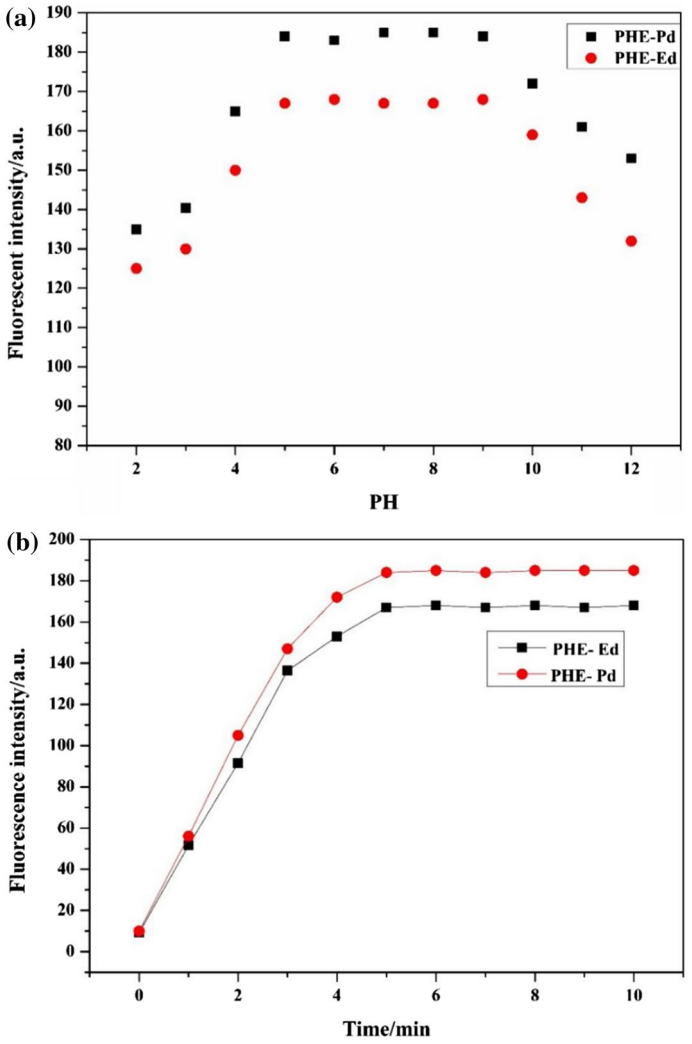

Fig. 10 **a** Effect of pH on the fluorescence intensity of **PHE–Ed** and **PHE–Pd** (10^{-5} M) in the presence of 10 μM Hg^{2+}; **b** Effect of response time on the fluorescence intensity of **PHE–Ed** and **PHE–Pd** (10^{-5} M) in the presence of 10 μM Hg^{2+}

Furthermore, the practical application of **PHE-Ed** and **PHE-Pd** for detection of Hg^{2+} was investigated in real samples including drinking water. As shown in Fig. 12, addition of the synthetic probes to drinking water containing Hg^{2+} resulted in color changes from colorless to light yellow, which indicated that the two probes showed potential applications in environmental samples.

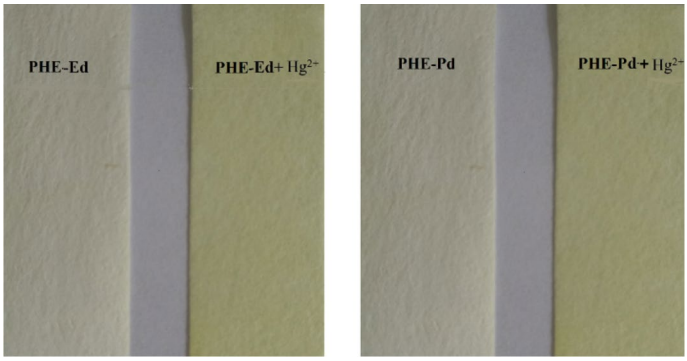

Fig. 11 The filter paper test strips of **PHE–Ed** and **PHE–Pd** in DMSO, treated with Hg^{2+} solution (10^{-5} M) in water

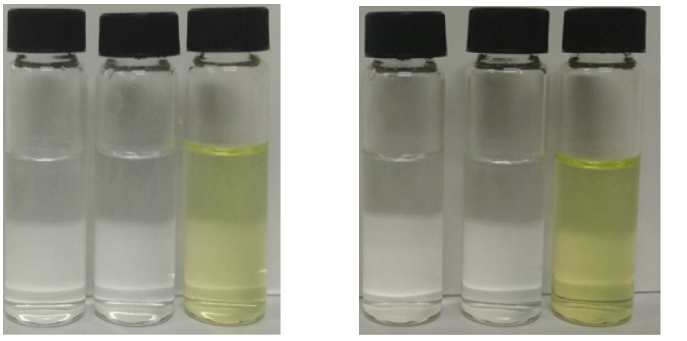

Fig. 12 The color change of **PHE-Ed** and **PHE-Pd** in real samples of drinking water (DW)

Compared with other probes

Finally, a detailed comparison between probes PHE-Ed and PHE-Pd and some other Hg^{2+}-selective fluorescent probes reported in the literature are represented in Table 1. Obviously, probes PHE-Ed and PHE-Pd showed high performances including superior DL, similar or even superior response time and pH response range in most cases compared with the previously reported probes [10, 12, 15, 33–37]. In addition, these two probes also exhibited excellent detection methods such as colorimetric, fluorescence in environmentally friendly aqueous EtOH media, which indicated that the two probes could be used to detect trace amounts of hazardous Hg^{2+} ions in real samples.

Table 1 Comparison of **PHE-Ed** and **PHE-Pd** for Hg^{2+} detection with other Hg^{2+}-selective probes

Structure of sensors	DL (nM)	Medium(v/v)	Response time	pH range	References
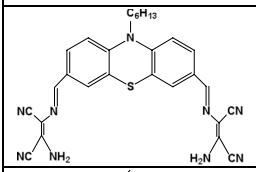	35	EtOH/H_2O(7/3)	No date	No date	[10]
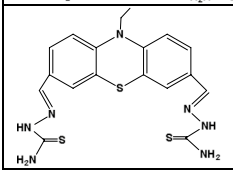	No date	HEPES buffer	No date	5–11	[15]
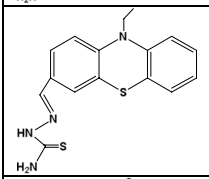	15	EtOH/H_2O(7/3)	No date	No date	[12]
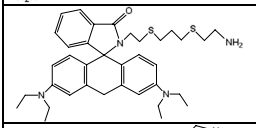	50	Dichcoromethance	No date	No date	[33]
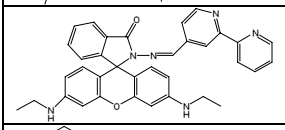	500	CH_3CN/H_2O(9/1)	No date	4.5–7.8	[34]
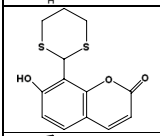	No date	EtOH/H_2O(8/2)	5 min	7.8–11.9	[35]
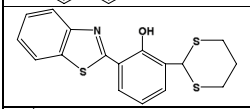	200	EtOH/H_2O(1/1)	15 min	3.0–6.0	[36]
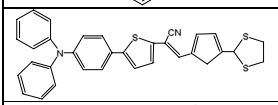	800	THF	6 min	No date	[37]
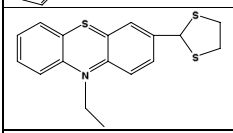	18.7	EtOH /H_2O(1/1)	5 min	5–11	This work
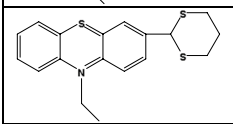	20.7	EtOH /H_2O(1/1)	5 min	5–11	This work

Conclusions

Two novel colorimetric fluorescent probes based on phenothiazine were designed and synthesized, and their detection ability toward Hg^{2+} was caused by the Hg^{2+}-promoted deprotection of thioacetal groups. The two probes exhibited high anti-interference performance, rapid response, high sensitivity and excellent selectivity towards Hg^{2+} within a wide pH range, and traces of Hg^{2+} ions could be rapidly detected in aqueous solution. Their recognition ability was tested on filter paper test strips and drinking water, and the results illustrated that the two probes could act as efficient solid–state colorimetric fluorescent probes for highly selective and sensitive detection of Hg^{2+}. It also illustrated that Hg^{2+} ions could be rapidly detected in drinking water by the two probes with high selectivity.

Acknowledgements The work was supported by the Shandong Provincial Natural Science Foundation of China (ZR2016EMM13, ZR2017LC005, ZR2018PB007), the Major Science and Technology Innovation Project of Shandong Province (2018CXGC1107).

References

1. A. Jiménez-Sánchez, N. Farfán, R. Santillan, Tetrahedron Lett. **54**, 39 (2013)
2. J. Ni, Q. Li, B. Li, L. Zhang, Sensor. Actuat. B-Chem. **186**, 186 (2013)
3. M. Üçüncü, E. Karakuş, M. Emrullahoğlu, Chem-Eur J. **21**, 38 (2015)
4. S. Li, H. Deng, W. Cao, C. Zhang, S. Jin, X. Xue, J. Zhang, F. Li, G. Zou, X.J. Liang, Analyst. **139**, 13 (2014)
5. C. Gong, D. Jiang, Q. Tang, L. He, X. Ma, C. Chow, Anal. Methods-UK **6**, 19 (2014)
6. H. Mi, M. Guan, J. Liu, H. Shan, Q. Fei, Y. Huan, G. Feng, Spectrochim. Acta. A. **176**, 168 (2017)
7. H. Zhang, Y. Huang, S. Hu, Q. Huang, C. Wei, W. Zhang, L. Kang, Z. Huang, A. Hao, J. Mater. Chem. C. **3**, 9 (2014)
8. K. Ma, X. Li, B. Xu, W. Tian, Anal. Methods-UK **6**, 7 (2014)
9. S.H. Mashraqui, T. Khan, S. Sundaram, S. Ghadigaonkar, Tterahedron Lett. **49**, 23 (2008)
10. K.M. Vengaian, C.D. Britto, K. Sekar, G. Sivaraman, S. Singaravadivel, RSC Adv. **6**, 9 (2016)
11. X. Hu, M.T. Tierney, M.W. Grinstaff, Bioconjugate Chem. **13**, 1 (2002)
12. K.M. Vengaian, C.D. Britto, G. Sivaraman, K. Sekar, S. Singaravadivel, RSC Adv. **5**, 115 (2015)
13. J. Weng, Q. Mei, B. Zhang, Y. Jiang, B. Tong, Q. Fan, Q. Ling, W. Huang, Analyst. **138**, 21 (2013)
14. S. Bishnoi, M.D. Milton, Tetrahedron Lett. **56**, 47 (2015)
15. W. Yang, S. Yang, Q. Guo, T. Zhang, K. Wu and Y. Hu, Sensor. Actuat. B-Chem. **213**, (2015)
16. X. Cheng, Q. Li, J. Qin, Z. Li, Acs Appl. Mater Inter. **2**, 4 (2010)
17. F. Lu, M. Yamamura, T. Nabeshima, Dalton T. **42**, 34 (2013)
18. X. Cheng, Q. Li, J. Qin, Z. Li, ACS Appl. Mater Inter. **2**, 4 (2010)
19. G.Q. Zhang, M. Xue, F.J. Huo, C.X. Yin, X.X. Yan, S. Jin, Chem. J. Chin. Uni. **34**, 9 (2013)
20. J. Park, B. In, K.H. Lee, RSC Adv. **5**, 69 (2015)
21. O.G. Nikolaeva, E.N. Shepelenko, K.S. Tikhomirova, Y.V. Revinskii, A.D. Dubonosov, V.A. Bren, V.I. Minkin, Mendeleev Commun. **26**, 5 (2016)
22. P. Srivastava, S.S. Razi, R. Ali, R.C. Gupta, S.S. Yadav, G. Narayan, A. Misra, Anal. Chem. **86**, 17 (2014)
23. R. Roy, S. Rakshit, S. Bhar, S.C. Bhattacharya, RSC Adv. **5**, 83 (2015)
24. R. Satapathy, Y.H. Wu, H.C. Lin, Org. Lett. **14**, 10 (2012)
25. R.L. Liu, H.Y. Lu, M. Li, S.Z. Hu, C.F. Chen, RSC Adv. **2**, 10 (2012)
26. K. Wang, S. Huang, Y. Zhang, S. Zhao, H. Zhang, Y. Wang, Chem. Sci. **4**, 8 (2013)

27. N. Dash, A. Malakar, M. Kumar, B.B. Mandal and G. Krishnamoorthy, Sensor. Actuat. B-Chem. 202, (2014)
28. S. Goswami, K. Aich, S. Das, M.C. Das, D. Sarkar, T.K. Mondal, Dalton T. **44**, 12 (2015)
29. T. Wei, J. Wang, Y. Chen, Y. Han, RSC Adv. **5**, 70 (2015)
30. X. Peng, Y. Xu, S. Sun, Y. Wu, J. Fan, Org. Biomol. Chem. **5**, 2 (2007)
31. X. Yang, R. Lu, H. Zhou, P. Xue, F. Wang, P. Chen, Y. Zhao, J. Colloid Interface Sci. **339**, 2 (2009)
32. S. Li, B. Zhao, W. Kan, L. Wang, B. Song, S. Chen, Res. Chem. Intermediat. **44**, 1 (2018)
33. M. Wang, F. Yan, Y. Zou, L. Chen, N. Yang, X. Zhou, Sensor. Actuat. B-Chem. **192**, 192 (2014)
34. D. Ding, J. Wang, Synth. React. Inorg. M. **46**, 4 (2016)
35. J. Hu, Z. Hu, S. Liu, Q. Zhang, H.W. Gao, K. Uvdal, Sensor. Actuat. B-Chem .230 (2016)
36. F. Lu, M. Yamamura, T. Nabeshima, Dalton T. **42**, 34 (2013)
37. H. Li, H. Yan, J. Phys. Chem. C **113**, 18 (2009)